PLOS ONE

RESEARCH ARTICLE

Preparation of Activated Carbon From *Polygonum orientale* Linn. to Remove the Phenol in Aqueous Solutions

Jia Feng, Shengli Shi, Liangyu Pei, Junping Lv, Qi Liu, Shulian Xie*

School of Life Science, Shanxi University, Taiyuan, China

* xiesl@sxu.edu.cn

Citation: Feng J, Shi S, Pei L, Lv J, Liu Q, Xie S (2016) Preparation of Activated Carbon From *Polygonum orientale* Linn. to Remove the Phenol in Aqueous Solutions. PLoS ONE 11(10): e0164744. doi:10.1371/journal.pone.0164744

Editor: Shaojun Dai, Northeast Forestry University, CHINA

Received: July 20, 2016

Accepted: September 29, 2016

Published: October 14, 2016

Data Availability Statement: All relevant data are within the paper.

Funding: The work was supported by Social Development Foundation of Shanxi (no. 201603D321001 to Jia Feng). The funders had no role in study design, data collection and analysis, decision to publish, or preparation of the manuscript.

Competing Interests: The authors have declared that no competing interests exist.

Abstract

Phenol components are major industry contaminants of aquatic environment. Among all practical methods for removing phenol substances from polluted water, activated carbon absorption is the most effective way. Here, we have produced low-cost activated carbon using *Polygonum orientale* Linn, a wide spreading species with large biomass. The phenol adsorption ability of this activated carbon was evaluated at different physico-chemical conditions. Average equilibrium time for adsorption was 120 min. The phenol adsorption ability of the *P. orientale* activated carbon was increased as the pH increases and reached to the max at pH 9.00. By contrast, the ionic strength had little effect on the phenol absorption. The optimum dose for phenol adsorption by the *P. orientale* activated carbon was 20.00 g/L. The dominant adsorption mechanism of the *P. orientale* activated carbon was chemisorption as its phenol adsorption kinetics matched with the pseudo-second-order kinetics. In addition, the equilibrium data were fit to the Langmuir model, with the negative standard free energy and the positive enthalpy, suggesting that adsorption was spontaneous and endothermic.

Introduction

Phenol is one of human carcinogen with characteristic pungent smell and taste. Although with low solubility in water, low amount of phenol components could severely affect human and aquatic organisms' gastrointestinal system and thus cause nausea, erythema, deep necrosis [1, 2]. Phenol substance is one of the major contaminants in the aquatic environment of from many modern industries, such as the coal conversion, dye manufacturing, papermaking, pesticide, petrochemical, pharmaceutical, and textile industries, etc [2]. It has been listed as one of the US Environmental Protection Agency priority pollutants [2, 3]. Attention has been increasingly concentrated on controlling phenol substances from industrial wastewater for decades, and limits have been placed on the amounts of phenol discharged, to attempt to ameliorate the direct and potentially negative impacts of phenol on the aquatic environment [4, 5]. There are various chemical, physical, physicochemical, and biological methods used to remove phenol from wastewater [6, 7], such as distillation [8], extraction with membrane adsorption [9],

microbial degradation [10], and oxidation using ozone [11], hydrogen peroxide, and chlorine oxides [7]. Among all these methods, adsorption has been proven to be the most effective and economic way for removing phenol from wastewater [2]. Activated carbon is the best and most common choice, which possesses excellent phenol adsorption ability [12–14]. Comparing to traditional physical activation for generating activated carbon, chemical activation presents several advantages, including single-step activation, low activation temperatures, low activation time, and better porous structure [15]. Thus, numerous attempts have been done to produce low-cost activated carbon for use in adsorptive dephenolation processes using a wide range of agricultural waste products[2, 16], such as nutshells, wood, fruit stones and so on. The agricultural wastes, including corn cobs, banana piths, oil palm, have been utilized as a precursor for the preparation of activated carbon [2, 3, 17].

Polygonum orientale Linn. is an annual herbage commonly occurred in freshwater wetlands [18, 19]. It grows rapidly and produces large quantities of biomass, which is usually used to construct wetlands for wastewater treatment [17]. This plant has porous caudex system and the texture is between medium hard to soft. Its mass of carbon is about 40–45%, volatiles mass is 58–60%, and the density is 0.50–0.60 cm^3/g. Thus, it could be considered to produce an effective activated carbon [20]. The potential capabilities of *P. orientale* in phytoremediation, especially of phenol, have been little reported [16].

In this study, we aimed to evaluate the potential for using activated carbon produced from *P. orientale* to remove phenol in aqueous solutions. The influences of several operating parameters, such as the initial phenol concentration, adsorbent dose, initial solution pH, and temperature, on the adsorption of phenol were examined in batch tests. Pseudo-first-order, pseudo-second-order, and diffusion kinetics models were used to identify the possible mechanisms involved in the adsorption process, and the Langmuir and Freundlich equations were used to analyze the adsorption equilibrium.

Materials and Methods

Preparation of *Polygonum orientale*

The *Polygonum orientale* was collected from Fenhe, Shanxi Province, China. The sampling site is a public area and no specific permission was required. And there is no endangered or protected species in our sampling area. The material was cut into small pieces of 2–3 cm and washed with distilled water to remove the water soluble impurities. Then they were dried in an air drying oven (101A-3, Suoyu, Shanghai, China) at 80°C for 6 h to get rid of the moisture and other volatile. The dried material was grounded into powder using an HR-1727 grinder (Philips, Zhuhai, China) and sieved through standard sieves to give 70–100 μm mesh particles.

The Brunauer Emmett Teller (BET) surface area and pore characteristics of *P. orientale* were measured by the surface area and pore analyzer (ASAP2020, Micromeritics, USA), under nitrogen adsorption at 77K.

The infrared spectroscopy was determined wave number from 400–4,000 cm^{-1} by Fourier transforms infrared (FTIR) spectrometer (AVATAR 370, Thermo Nicolet, USA). Consequently, the numbers of surface groups on *P. orientale* were determined by titration method [21].

Adsorption experiments

Stock solution containing phenol at a concentration of 1000 mg/L was prepared. Experimental solutions with gradient concentrations of phenol were prepared by diluting the stock solution. The adsorption effects at different conditions (contact times, shaking rates, temperatures, solution pH values, and ionic strengths) were examined. The experiments were performed using a

temperature-controlled water bath shaker (HH-2, Guohua, Beijing, China). The initial pH of each experimental solution was adjusted to the desired value by adding $HCl_{(aq)}$ or $NaOH_{(aq)}$. The ionic strength of each solution was adjusted by adding NaCl and $MgCl_2$.

In brief, the adsorption experiments were performed by shaking 2.00 g of *P. orientale* powder with 100 mL of the experimental solution containing a known concentration of phenol in the temperature-controlled water bath shaker. The mixture was continuously mixed, with a constant agitation speed of 120 rpm (using a 78–1 mixing instrument, Jintanhuanyu, Jiangsu, China). After the absorpting, the solution was filtered and the remaining phenol concentration was determined by OD_{270} using UV/visible spectrophotometer (SP-752PC, Guangpu, Shanghai, China). The phenol uptake at equilibrium q_e (mg/g) and the percentage of phenol removed from the solution (Adsorption%) were calculated using Eqs (1) and (2), respectively,

$$q_e = \frac{(C_0 - C_e)V}{W}, \tag{1}$$

$$\text{Adsorption}(\%) = \frac{C_0 - C_e}{C_0} \times 100, \tag{2}$$

where C_0 and C_e (mg/L) are the initial and equilibrium phenol concentrations, respectively, V (L) is the volume of the solution, and W (g) is the mass of adsorbent used.

Adsorption kinetics model

Two different kinetics models were applied to the experimental data to allow the kinetics of the adsorption of phenol onto the *P. orientale* powder to be evaluated.

Pseudo-first-order model. The pseudo-first-order equation Eq (3) has been widely used to describe the adsorption of an adsorbate in an aqueous solution onto an adsorbent. This equation is based on the assumption that the rate of change in the uptake of a solute by an adsorbent over time is directly proportional to the change in the difference between the saturation concentration and the amount of solute that is adsorbed over time [22].

$$\frac{dq_t}{dt} = k_1(q_e - q_t) \tag{3}$$

When $q_t = 0$ at $t = 0$, Eq (3) can be integrated to give Eq (4),

$$\log(q_e - q_t) = \log q_e - \frac{k_1}{2.303}t, \tag{4}$$

in which q_e and q_t (mg/g) are the amounts of phenol adsorbed at equilibrium and at time t, respectively, t (min) is the contact time, and k_1 (1/min) is the rate constant for this equation. The values of k_1 and q_e can be calculated from a plot of log (q_e–q_t) against t.

Pseudo-second-order model. The pseudo-second-order kinetics equation [23] can be presented as shown in Eq (5).

$$\frac{dq_t}{dt} = k_2(q_e - q_t)^2 \tag{5}$$

On integrating Eq (5) and noting that $q_t = 0$ at $t = 0$, the equation can be rearranged into the linear form shown in Eq (6),

$$\frac{t}{q_t} = \frac{1}{k_2 q_e^{\,2}} + \frac{1}{q_e}t, \text{ where } \mathrm{h} = k_2 q_e^{\,2}, \tag{6}$$

where h (mg/(g min)) is the initial adsorption rate and k_2 (g/(mg min)) is the pseudo-second-order rate constant. The values of q_e, k_2, and h can be obtained from a linear plot of t/q_t against t.

Adsorption mechanism

The diffusion mechanism could not be identified using the pseudo-first-order and pseudo-second-order kinetics models. The intraparticle diffusion model was therefore used to gain insight into the mechanisms involved and to identify the rate-controlling step. This model described by Weber and Morriss [24], shown in Eq (7), can be used to gain insight into the mechanisms and rate-controlling steps that affect adsorption kinetics.

$$q_t = k_{pi} t^{1/2} + C_i \tag{7}$$

In Eq (7), k_{pi} (mg/ (g $\text{min}^{1/2}$)) is the intraparticle diffusion rate constant for stage i and C_i is the intercept for stage i. The C value gives information on the thickness of the boundary layer, with a larger intercept meaning that the boundary-layer effect is stronger. To use the intraparticle diffusion model, a plot of q_t against $t^{1/2}$ should give a straight line, with a slope of k_p and an intercept of C [14, 25].

Adsorption isotherms

The adsorption isotherm model is of fundamental importance to the description of the interactive behavior between an adsorbate and an adsorbent. The analysis of isotherm data is an important way for predicting the adsorption capacity and describing the surface properties of an adsorbent and the affinity of the adsorbent for the adsorbate of interest. The Langmuir and Freundlich isotherms were used to analyze the experimental equilibrium data for the sorption of phenol by the *P. orientale* powder in our study.

Langmuir isotherm. The Langmuir isotherm is based on the assumption that the adsorbent has a homogeneous structure and that all sorption sites are identical and energetically equivalent [26]. The Langmuir isotherm equation can be written as

$$\frac{C_e}{q_e} = \frac{1}{Q_m b} + \frac{1}{Q_m} C_e, \tag{8}$$

where C_e (mg/L) is the equilibrium concentration of the adsorbate, q_e (mg/g) is the amount of adsorbate adsorbed per unit mass of adsorbent, b (L/mg) is the Langmuir adsorption constant, and Q_m (mg/g) is the maximum amount adsorbed. A dimensionless constant separation factor or equilibrium parameter R_L can be defined using Eq (9) [27] to determine if adsorption is favorable.

$$R_L = \frac{1}{1 + bC_0} \tag{9}$$

In Eq (9), b (L/mg) is the Langmuir isotherm constant and C_0 (mg/L) is the initial phenol concentration. The R_L value indicates whether the isotherm is favorable ($0<R_L<1$), unfavorable ($R_L>1$), linear ($R_L = 1$), or irreversible ($R_L = 0$). The Langmuir constants can be obtained from a plot of C_e/q_e against C_e.

Freundlich isotherm. The Freundlich isotherm can be used to describe a heterogeneous system and reversible adsorption that is not restricted to the formation of a monolayer [28]. The Freundlich isotherm can be expressed in a linear form as

$$\log q_e = \log K_F + \left(\frac{1}{n}\right) \log C_e, \tag{10}$$

where K_F and n are Freundlich constants. K_F ((mg/g) (L/mg)$^{1/n}$) indicates the adsorption capacity of the adsorbent. A larger K_F value indicates that the adsorbent has a larger adsorption capacity. The value of n indicates how favorable the adsorption process is. A value of $1/n<1$ indicates a normal Friedrich isotherm and cooperative adsorption. The Freundlich constants can be obtained from a plot of log q_e against log C_e.

Adsorption thermodynamics

The change in standard free energy (ΔG; kJ/mol), enthalpy (ΔH; kJ/mol), and entropy (ΔS; kJ/(mol K)) can be determined using Eqs (11) and (12) [29].

$$\Delta G = -RT\ln K \tag{11}$$

$$\Delta G = \Delta H - T\Delta S \tag{12}$$

In these equations, R is the universal gas constant (8.314 kJ/(mol K)), T is the temperature (K), and K is the Langmuir constant (L/mol) obtained from a plot of C_e/q_e against C_e. The ΔH and ΔS values can be calculated from the slope and intercept of the line found by plotting ΔG against T.

Results and Discussion

Characterization of *Polygonum orientale*

The characteristics of the *Polygonum orientale* particle were shown in Table 1. The BET surface area was 1255.10 m^2/g, which was much higher than other various low cost activated carbons reported in literature [3, 30–32]. The BJH adsorption average pore diameter was 7.433 nm and the BJH adsorption average pore volume was 0.337 cm^3/g. For the pore analysis, the good surface area and the mesopore volume are an indication of effective adsorption of phenol on the adsorption.

According to the FTIR spectroscopy data, many surface organic functional groups of *P. orientale* have been identified (Fig 1), which was supposed to be responsible for phenol uptake. The characteristic band at 3421.63 cm^{-1} could be assigned to the–OH stretching vibration of hydroxyl functional groups including hydrogen bonding [33, 34]. The band at around 2920.50 cm^{-1} was ascribed to the asymmetric C–H stretching vibrations in aliphatic structure. The peaks occurring at 2363.90 cm^{-1} was due to C–O vibrations [2]. The band located at 1624.40 cm^{-1} was suggested to be C = C stretching in ethylene groups. The band at 1507.760 cm^{-1} was due to C = C stretching in aromatic group [2]. The peak occurring at 1384.19 cm^{-1} was ascribed to the C–H stretching. The band located at 1318.76 cm^{-1} represented C–O vibration in carboxylate group. The band at around 1255.26 cm^{-1} was due to the C–OH stretching vibrations in alcoholic groups and carboxylate group. The peak at 1059.04 cm^{-1} was ascribed C–H of the alcoholic groups and the carboxylic acids [24]. The band at around 833.39 (also 781.12) cm^{-1} was assigned to C–H twist vibrations in aromatic groups. The band located at 668.01 cm^{-1} attributed to O–H bending vibrations in alcohol and phenol groups. As stated by the possible functional groups assigned to the peak in FTIR spectra, the oxygen groups were the important

Table 1. Chemical characteristics of *Polygonum orientale*.

Sample	pH_{pzc}	Total basicity (mmol/g)	Total acidity (mmol/g)	Carboxyls (mmol/g)	Phenols (mmol/g)	Lactones (mmol/g)	Carbonyl (mmol/g)
P. orientalis	7.10	1.5300	1.5273	0.3167	0.7086	0.2000	0.3020

doi:10.1371/journal.pone.0164744.t001

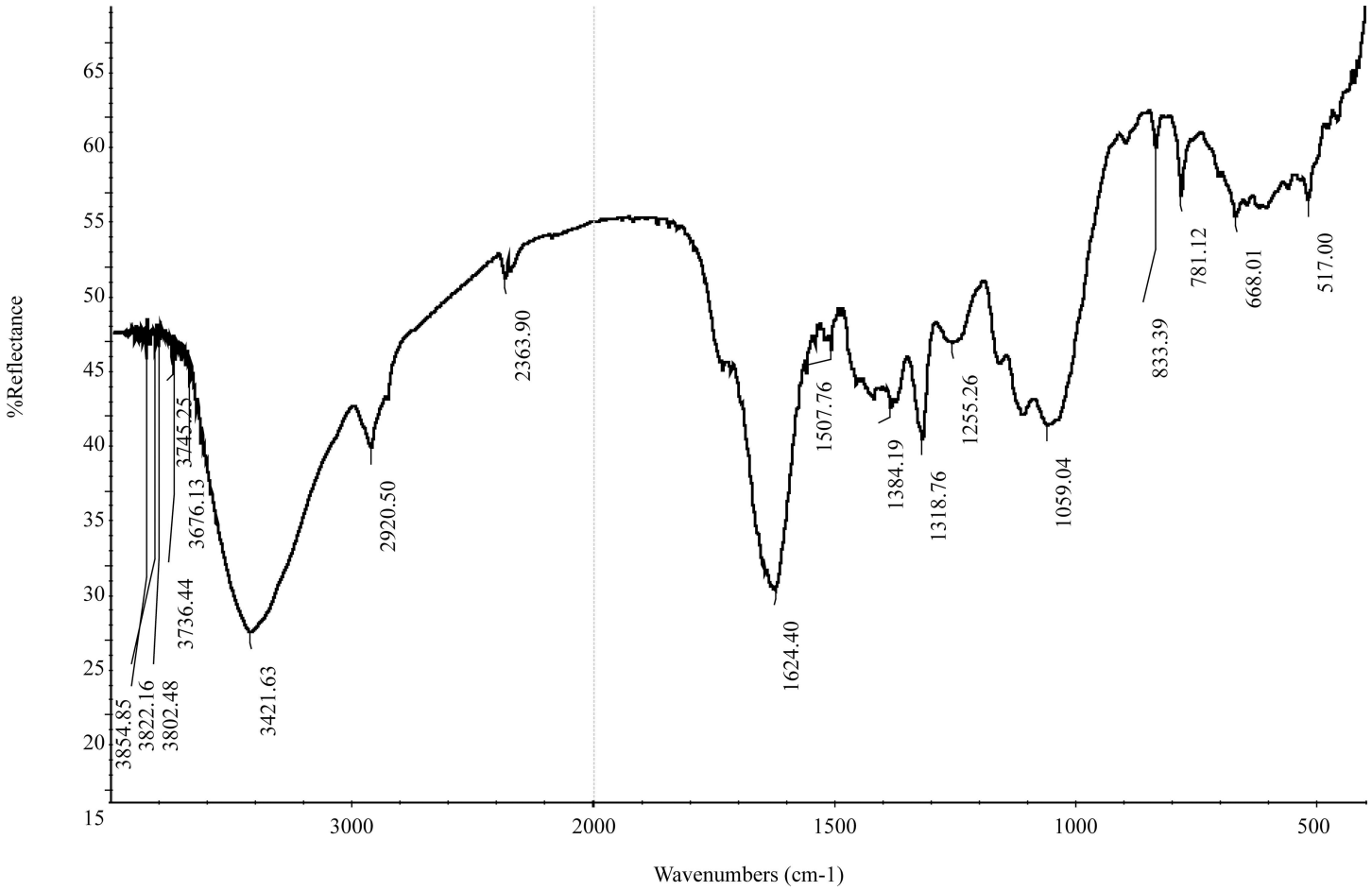

Fig 1. Fourier transform infrared spectra on *Polygonum orientale* surface.

doi:10.1371/journal.pone.0164744.g001

functional groups of *P. orientale*, which included ethers, esters, alcohols and phenol groups. In order to further clarify the chemistry portraits of the *P. orientale*'s surface, Boehm titration has been done (Table 1). *P. orientalis* has general equal acidic groups and basic ones on the surface. Thus, it could be considered that the *P. orientalis* activated carbon is neutral.

Effect of the initial phenol concentration, time, and temperature

The change in the amount of phenol adsorbed by the *P. orientale* powder over time (up to 200 min) was investigated. Phenol adsorption is significantly influenced by the initial concentration of phenol in aqueous feed solution. The higher initial concentration was used, the shorter time was taken to reach the equilibrium. Nevertheless, the equilibrium time for the lowest concentration, 50 mg/L, being tested in this study was 120 min. Therefore, the equilibrium time in our study was considered to be 120 min, as this time duration was sufficient for equilibrium to be reached at all three concentrations, 50 mg/L, 100 mg/L, and 150 mg/L (Fig 2A and 2B). As shown in the figure, the amount of phenol adsorbed increased as the initial phenol concentration increased in the first 100 min at room temperature. The rapid uptake at initial phase is due to the vacant adsorption sites making it easier for phenol interaction with these sites [35]. And in the initial phase, transport to the sites is also important for a reaction to be fast. The amount of phenol uptake remained constant after 120 min. The adsorption amount increased with an

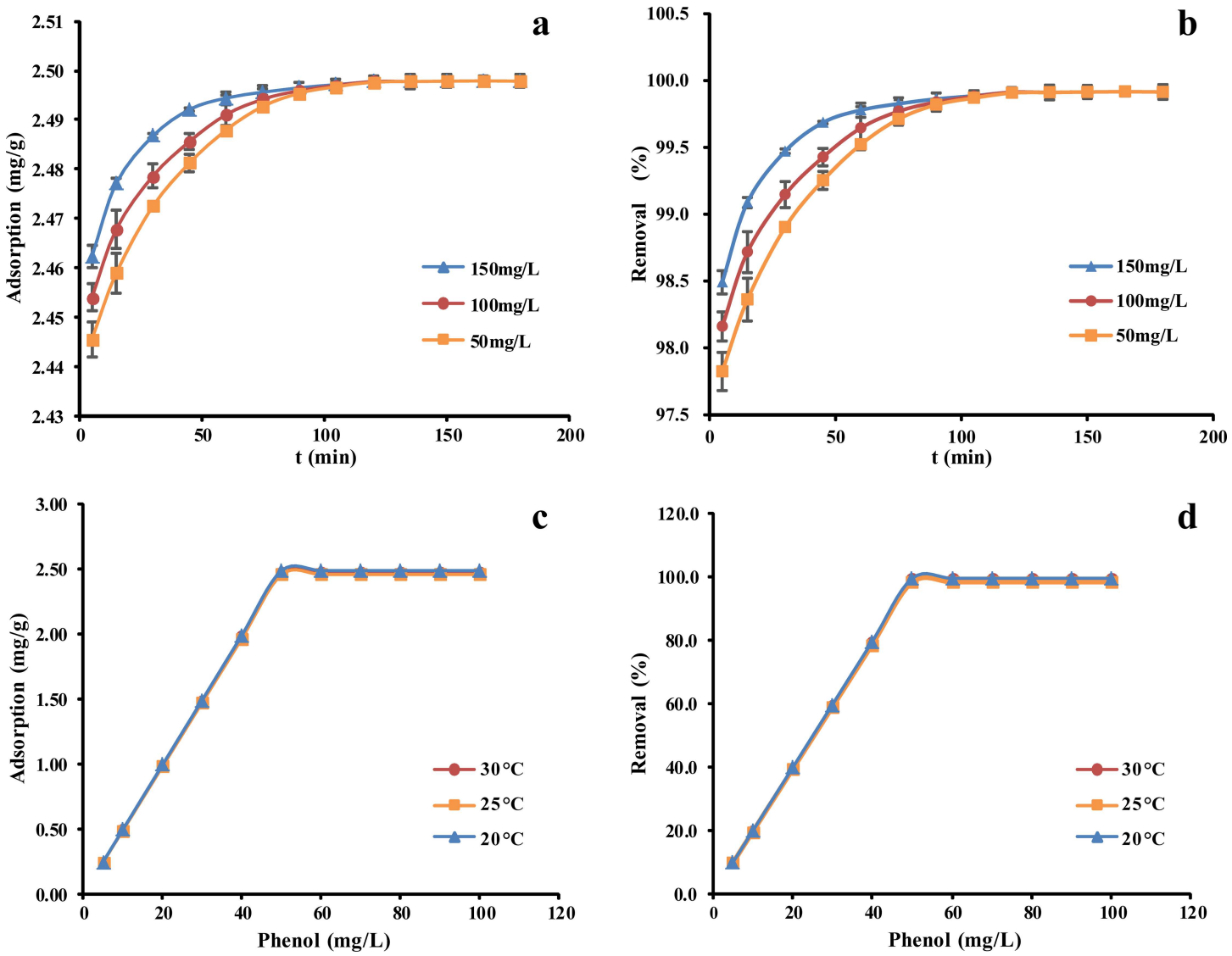

Fig 2. (a, b) Effect of adsorption equilibrium time and comparison (temperature = 25±1˚C), (c, d) equilibrium temperature and comparison of different phenol concentrations on *P. orientale* (*P. orientale* dosage = 20.00 g/L).

doi:10.1371/journal.pone.0164744.g002

increase in initial phenol concentration. It was due to that higher initial phenol concentration would have stronger driving force for the transferring the phenol from the aqueous phase to the solid phase and more collisions has occurred between phenol ions and the adsorbent surfaces [36].

The temperature variation is another important factor affecting the activated carbon adsorption. Since adsorption is an exothermic process, it is suggested that adsorption capacity normally decreases when temperature goes up [12]. However, the adsorption capacity of *P. orientale* activated carbon showed no changes at all three temperature conditions tested in this study (Fig 2C and 2D). As all three conditions were considered as room temperature, it could be concluded that the room temperature was the best option for adsorption by *P. orientale* activated carbon and little effects on the adsorption ability by temperature changing at room temperature range.

Effect of adsorbent dose

The influence of the adsorbent dose on the amount of phenol removed by the *P. orientale* powder is shown in Fig 3. The percentage of phenol removed from the solution increased from 25% to 98% as the *P. orientale* dose was increased from 5.00 g/L to 20.00 g/L, and then remained almost constant at higher doses of *P. orientale*. This was expected because the adsorbed phenol either blocked access to the initial pores or caused particle aggregation, thereby reducing the available active sites. Increasing the adsorbent dose has increased the surface area of the adsorbent in the test solution and thus the availability of adsorption sites [37]. The optimum *P. orientale* dose was found to be 20.00 g/L, as no obvious increase adsorption was seen with absorbent dose higher than 20.00 g/L.

Effect of pH

The effect of the pH on phenol clearance efficiency was assessed by absorption experiments at gradient pH conditions, from pH 2.00 and pH 12.00 (Fig 4A). The adsorption capacity for phenol increased as the initial pH was increased from a value of 2.00 to a value of 9.00, and the percentage of the phenol that was removed from the solution increased dramatically, from 91.30% to 96.30%. However, the percentage of the phenol that was removed decreased as the pH was increased from a value of 9.00 to a value of 11.00.

There were a great number of critical functional groups on the *P. orientale* surface according to Fig 1. The pH of phenol sorption from the aqueous depended on the type and ionic state of

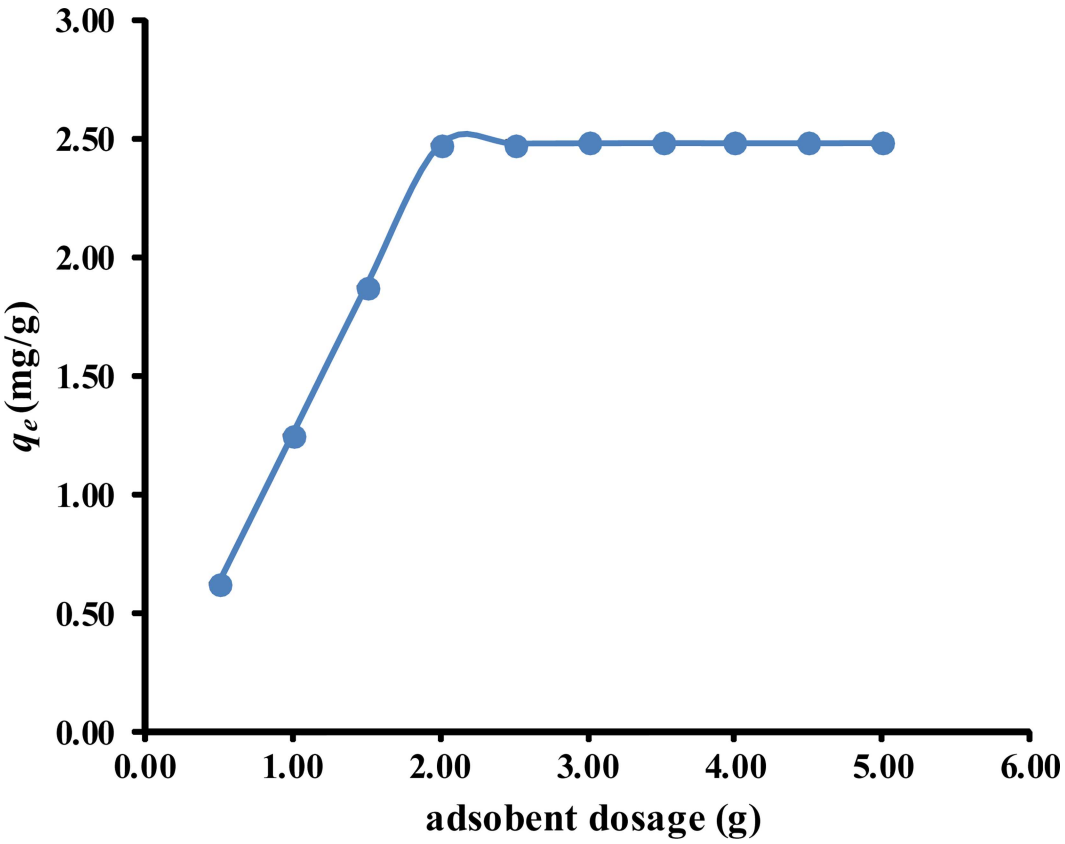

Fig 3. Effect of adsorbent dosage on adsorption of phenol by *P. orientale* (C_0 = 50 mg/L; *P. orientale* dosage = 20.00 g/L; temperature = 25±1˚C).

doi:10.1371/journal.pone.0164744.g003

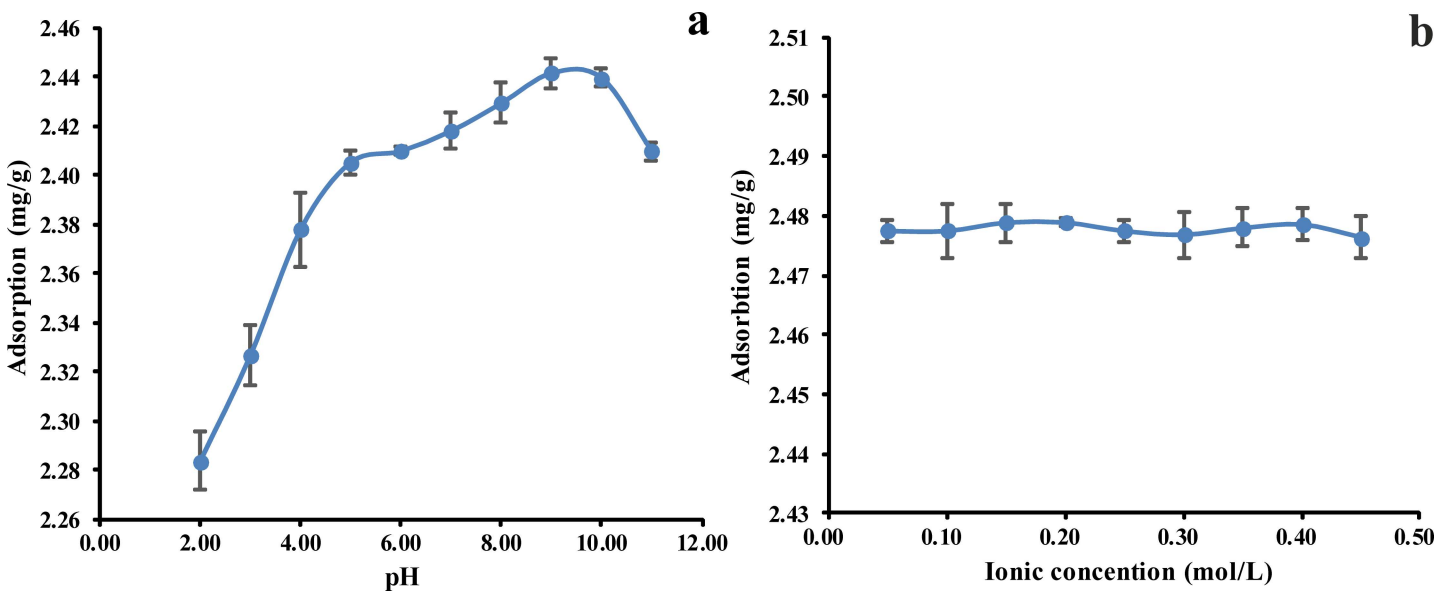

Fig 4. (a) Effect of pH value on adsorption of phenol by *P. orientale*, (b) ionic concentration on adsorption of phenol by *P. orientale* (C_0 = 50 mg/L; *P. orientale* dosage = 20.00 g/L; temperature = 25±1˚C).

doi:10.1371/journal.pone.0164744.g004

the functional groups and the phenol chemistry [2]. Both the phenol and the surface groups coexist in their protonated and deprotonated forms without buffered solutions, depending on the pK_a (= 9.89) values of phenol [12]. The phenol adsorption was decreased from pH 9.00 to pH 2.00, because of the decreased H^+ adsorption on the carbonyl sites and suppressed phenol adsorption on these sites. At the acidic pH, both the functional groups on the carbon surface and the phenolic compounds were in the non-ionized forms, pH<pK_a. The surface groups are either neutral or positively charged. As the initial solution pH increased, the number of negatively charged active sites increased while the number of positively charged sites decreased. The strength of the electrostatic repulsion between an adsorbent site and a positively charged phenol ion therefore decreased, which could result in more adsorption occurring. Less phenol has been adsorbed by the *P. orientale* powder at acidic pH values because of competition between the excess hydrogen ions in the solution and the *P. orientale* ions available as adsorption sites [32, 38, 39]. At weak alkaline pH values, the presence of OH^- ions promotes the transformation of the phenol molecules into the ionic state. This could explain the highest adsorption capacity and highest adsorption rate found at weakly alkaline pH values (i.e., at relatively low OH^- concentrations). At a value pH = 11.00 (for pH>pKa), the phenol dissociates, and forms phenolate anions, while the surface functional groups are either neutral or negatively charged. The electrostatic repulsion between the *P. orientale* material and the phenol ions would lead to the decrease of the amount of phenol adsorbed [32, 40].

Effect of ionic strength

The effect of changing the ionic strength of the solution on the amount of phenol adsorbed was measured, and plots of the amounts of phenol adsorbed against the NaCl concentrations used are shown in Fig 4B. The amount of phenol adsorbed by *P. orientale* and the adsorption rate did not vary in any clear way as the ionic strength was changed. As described by Lützenkirchen [41], two different surface complexes, inner-sphere and outer-sphere complexes, can form during the sorption process. In inner-sphere surface complexes covalent bonds form between the

Table 2. Pseudo-first-order and pseudo-second-order kinetic equation.

C_e (mg/L)	Pseudo-first-order		Pseudo-second-order	
50	y = -0.0188 x—1.0335	R^2 = 0.9540	y = 0.3996x + 0.1101	R^2 = 0.9999
100	y = -0.0199 x—1.1062	R^2 = 0.9347	y = 0.3998 x + 0.0839	R^2 = 0.9999
150	y = -0.0188 x—1.3461	R^2 = 0.9537	y = 0.3999 x + 0.0512	R^2 = 0.9999

doi:10.1371/journal.pone.0164744.t002

adsorbed molecules or ions and the surface functional groups, whereas no covalent bonds form in outer-sphere surface complexes. Non-covalent interactions, such as electrostatic attraction, hydrogen bonding, or hydrophobic attraction, are therefore responsible for the adsorption of adsorbate species in outer-sphere complexes. It has been assumed that insensitivity to the ionic strength indicates that inner-sphere surface complexes are formed, and that a decrease in the amount of adsorbate adsorbed as the ionic strength increases indicates that outer-sphere surface complexes are formed. The independence of the adsorption of phenol by the *P. orientale* material in our study could therefore be explained by inner-sphere complexes forming between the phenol and the *P. orientale* material [42, 43].

Adsorption kinetics

The kinetics parameters found for the adsorption of phenol by the *P. orientale* material are shown in Tables 2 and 3. The R^2 value obtained for the pseudo-first-order kinetics model was relatively low, and the calculated q_e (cal) values were much lower than the experimental q_e (exp) values (Fig 5A). However, the experimental results fitted the pseudo-second-order model well, with an extremely high R^2 value of 0.9999 (i.e., close to unity). Moreover, the experimental q_e (exp) values agreed well with the calculated values (Fig 5B). These results indicate that the adsorption of phenol by the *P. orientale* material followed the pseudo-second-order kinetics model. This means that the adsorption mechanism could depend on the concentrations and characteristics of both the adsorbate and the adsorbent [44], and that the rate limiting step might be chemisorption involving valence forces caused by the sharing or exchange of electrons [43, 45].

Adsorption mechanism

The diffusion mechanism could not be identified using the pseudo-first-order and pseudo-second-order kinetics models. The intraparticle diffusion model was therefore used to gain insight into the mechanisms involved and to attempt to identify the rate-controlling step.

The amounts of phenol adsorbed compared with the $t^{1/2}$ values for the intraparticle transport of phenol by *P. orientale* for different initial phenol concentrations are shown in Fig 6. The plots are multilinear with three portions, each of which is for a different stage in the adsorption process. The first portion, with the steepest slope, is the external mass transfer stage. The second portion is the gradual adsorption stage, in which intraparticle diffusion is the rate-limiting step. The third portion is the final equilibrium stage, in which intraparticle

Table 3. Pseudo-first-order and pseudo-second-order kinetic parameters.

C_e (mg/L)	Pseudo-first-order model				Pseudo-second-order model	
	q_e(exp) (mg/g)	$k_1 \times 10^{-2}$ (min^{-1})	q_e(cal) (mg/g)	k_2 (g/mg·min)	q_e(cal) (mg/g)	h (mg/g·min)
50	2.4979	4.3189	0.0926	1.4499	2.5024	9.0793
100	2.4979	4.5967	0.0783	1.9054	2.5015	11.9223
150	2.4979	4.3298	0.0451	3.1236	2.5001	19.5239

doi:10.1371/journal.pone.0164744.t003

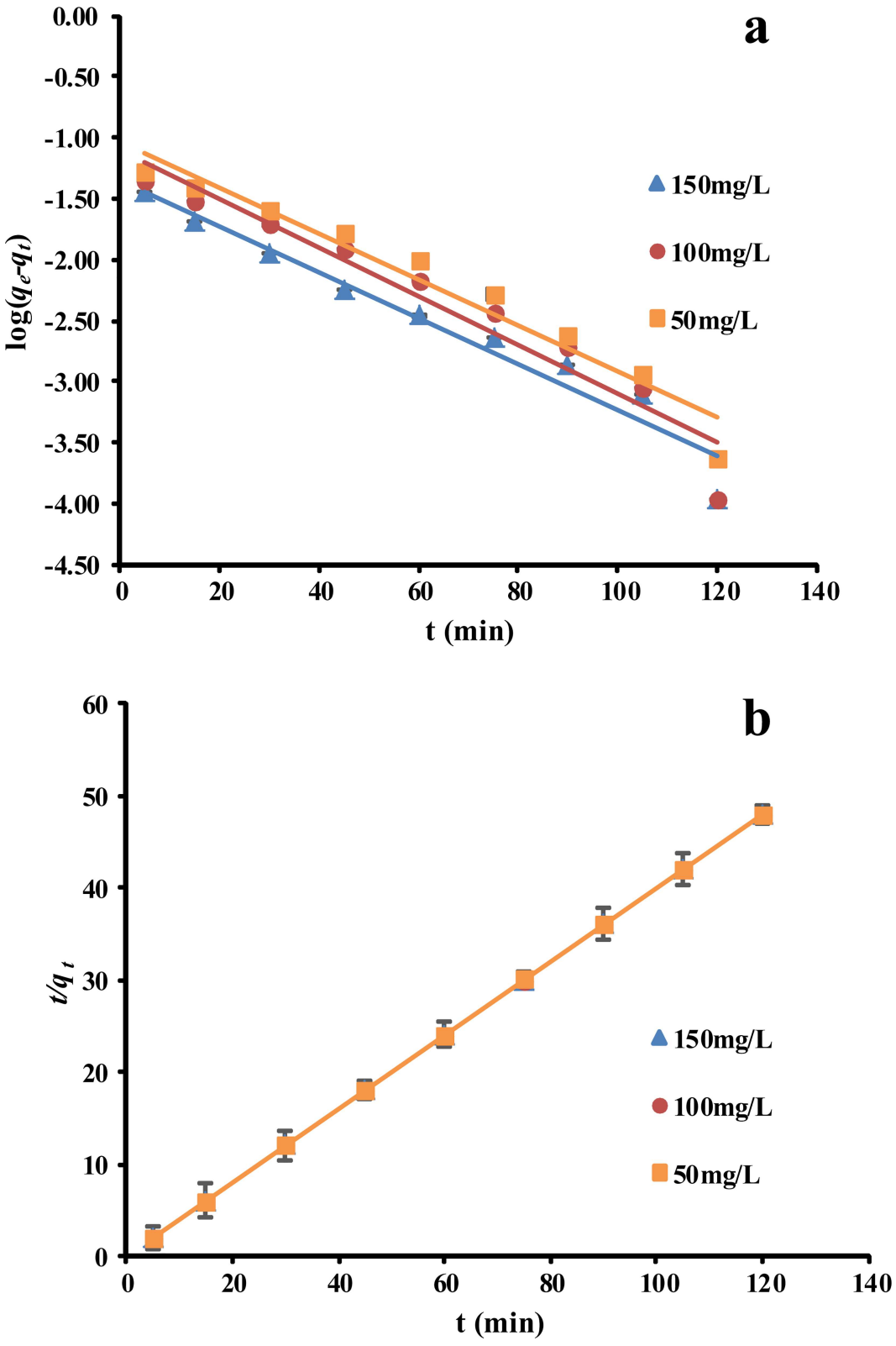

Fig 5. (a) Pseudo-first-order kinetics plots on adsorption of phenol by *P. orientale*, (b) Pseudo-second-order kinetics plots on adsorption of phenol by *P. orientale* (C_0 = 50 mg/L; *P. orientale* dosage = 20.00 g/L; temperature = 25±1˚C).

doi:10.1371/journal.pone.0164744.g005

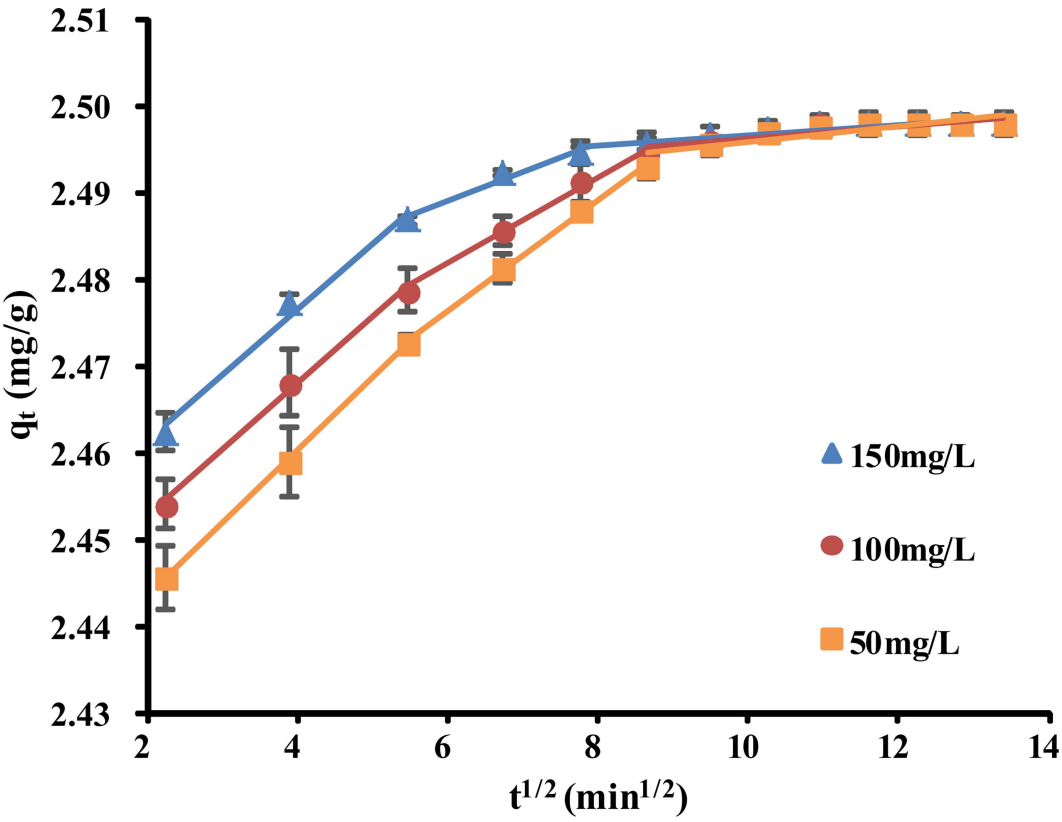

Fig 6. Intraparticle diffusion plots for adsorption of phenol on by *P. orientale* (C_0 = 50, 100, 150 mg/L; *P. orientale* dosage = 20.00 g/L; temperature = 25±1˚C).

doi:10.1371/journal.pone.0164744.g006

diffusion starts to slow down because of the extremely low adsorbate concentration remaining in the solution [32, 46]. The lines do not pass through the origin, so we can conclude that intra-particle diffusion is not the only rate-limiting step and that boundary layer control may be involved in the process [47]. Some other mechanisms, such as the formation of complexes or ion exchange, may also exert some control over the adsorption rate [48]. The model parameters defined in the equation described are given in Table 4. The *C* values increased as the initial phenol concentration increased and K_{pi} decreased. This indicates that the rate at which phenol was removed was higher at the beginning of the adsorption tests because of the large surface area of the adsorbent that was available to adsorb phenol.

Adsorption isotherms

Plots of q_e against C_0 for the adsorption of phenol onto *P. orientale* at 20°C, 25°C, and 30°C are shown in Fig 7A and 7B, according to the Langmuir and Freundlich isotherms, respectively.

Table 4. Intra-particle diffusion parameters.

C_0(mg/L)	Intra-particle diffusion model								
	k_{p1} (mg/gmin$^{1/2}$)	k_{p2} (mg/gmin$^{1/2}$)	k_{p3} (mg/gmin$^{1/2}$)	C_1	C_2	C_3	$(R_1)^2$	$(R_2)^2$	$(R_3)^2$
50	0.0083	0.0064	0.0009	2.4269	2.438	2.4863	0.9999	0.9957	0.7301
100	0.0086	0.005	0.0007	2.4375	2.452	2.4894	0.9954	0.9901	0.7394
150	0.0076	0.0034	0.0006	2.4462	2.4684	2.4907	0.9859	0.9695	0.833

doi:10.1371/journal.pone.0164744.t004

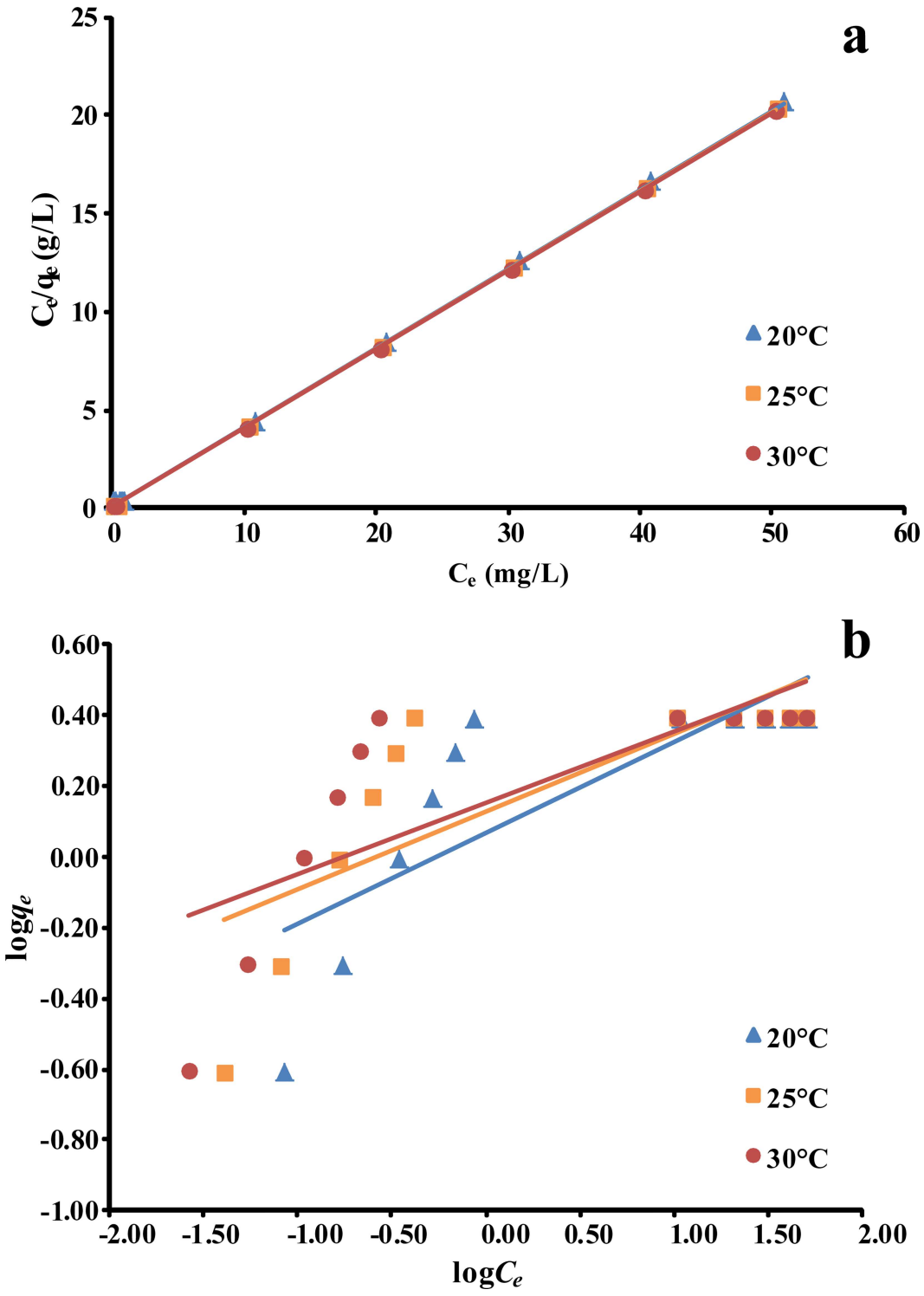

Fig 7. (a) Langmuir isotherm for adsorption of phenol onto *P. orientale* at different temperatures, (b) Freundlich isotherm for adsorption of phenol onto *P. orientale* at different temperatures (temperature = 20, 25, 30˚C; C_0 = 5–100 mg/L; *P. orientale* dosage = 20.00 g/L)

doi:10.1371/journal.pone.0164744.g007

Table 5. Langmuir and Freundlich isotherm equation.

T (K)	Langmuir equation		Freundlich equation	
293	y = 0.4030 x + 0.1501	R^2 = 0.9999	y = 0.2597 x + 0.0679	R^2 = 0.6229
298	y = 0.4014 x + 0.0702	R^2 = 0.9999	y = 0.2199 x + 0.1271	R^2 = 0.5920
313	y = 0.4009 x + 0.0454	R^2 = 0.9999	y = 0.2015 x + 0.1531	R^2 = 0.5770

doi:10.1371/journal.pone.0164744.t005

Table 6. Isotherm model constants of four isotherm models for phenol adsorption onto *P. orientale*.

T (K)	Langmuir model parameters			Freundlich model parameters	
	Q_m (mg/g)	b (L/mg)	R_L	K_F (mg/g(L/mg)$^{1/n}$)	1/n
293	2.4816	16.5277	0<R_L<1	1.1692	0.2597
298	2.4912	35.4996	0<R_L<1	1.3399	0.2199
313	2.4943	54.9778	0<R_L<1	1.4227	0.2015

doi:10.1371/journal.pone.0164744.t006

Table 7. Thermodynamic parameters for the adsorption of phenol onto *P. orientale* at different temperatures.

T (K)	Thermodynamic equation: y = -162.59x + 40294, R^2 = 0.8827		
	ΔG (kJ/mol)	ΔH (kJ/mol)	ΔS (kJ/mol K)
293	-6.833	40.294	-0.162
298	-8.843		
313	-10.427		

doi:10.1371/journal.pone.0164744.t007

The values for the constants calculated using the two isotherms are given in Tables 5 and 6. The adsorption of phenol onto *P. orientale* fitted the Langmuir isotherm model well, giving high R^2 values (0.9998–0.9999). This may have been caused by the homogeneous distribution of active sites on the surfaces of the *P. orientale* material. Furthermore, the R_L values for the Langmuir isotherm were between zero and one, but the Freundlich constant $1/n$ was lower than one, indicating that adsorption was favorable. The maximum adsorption capacity Q_m increased as the temperature increased, showing that the process was endothermic. The high adsorption capacity found in this study revealed that *P. orientale* is a promising adsorbent for removing phenol from aqueous solutions.

Adsorption thermodynamics

The adsorption thermodynamics results are given in Table 7. A positive ΔH value was found, further confirming that the adsorption process was endothermic. ΔG was negative, reflecting the spontaneity and feasibility of the adsorption process.

Conclusions

The present work showed that *P. orientale* could be used as an good adsorbent for the removal of phenol in aqueous solutions. The amount of phenol adsorbed depended strongly on the contact time, pH, adsorbent dose, and temperature, but not ionic strength. More phenol was adsorbed as the pH increased, the optimum being pH 9.0. The optimum adsorbent dose was 20.0 g/L. Equilibrium was reached in 120 min. Adsorption followed pseudo-second-order kinetics, so the dominant process was chemisorption. The equilibrium data were well described by the Langmuir model. ΔG was negative and ΔH was positive, meaning adsorption was

spontaneous and endothermic. There is great potential for using *P. orientale* as an economical and efficient adsorbent for removing phenol from aqueous solutions.

Acknowledgments

We are grateful to Edanz Editing company for the editorial assistance with the English.

Author Contributions

Conceptualization: JF JL QL SX.

Formal analysis: JF SS LP.

Investigation: JF SS LP JL QL SX.

Resources: JF SS LP SX.

Writing – original draft: JF SS LP.

Writing – review & editing: JF JL QL SX.

References

1. Jha P, Jobby R, Kudale S, Modi N, Dhaneshwar A, Desai N. Biodegradation of phenol using hairy roots of *Helianthus annuus* L. Intern Biodet Biodegr. 2013; 77: 106–113.
2. Nath K, Panchani S, Bhakhar MS, Chatrola S. Preparation of activated carbon from dried pods of *Prosopis cineraria* with zinc chloride activation for the removal of phenol. Environ Sci Pollut Res. 2013; 20: 4030–4045.
3. Sathishkumar M, Binupriya AR, Kavitha D, Selvakumar R, Jayabalan R, Choie JG, et al. Adsorption potential of maize cob carbon for 2, 4-dichlorophenol removal from aqueous solutions: equilibrium, kinetics and thermodynamics modeling. Chem Eng J. 2009; 147: 265–271.
4. Ahluwalia SS, Goyal D. Microbial and plant derived biomass for removal of heavy metals from wastewater. Bioresour Technol. 2007; 98: 2243–2257. doi: 10.1016/j.biortech.2005.12.006 PMID: 16427277
5. Coniglio MS, Busto VD, Gonzáles PS, Medina MI, Milrad S, Agostini E. Application of Brassica napus hairy root cultures for phenol removal from aqueous solutions. Chemosphere. 2008; 72: 1035–1042. doi: 10.1016/j.chemosphere.2008.04.003 PMID: 18499219
6. Kulkarni SJ, Kaware JP. Review on research for removal of phenol from wastewater. Int J Sci Res Public. 2013; 3: 1–5.
7. Rengaraj S, Moon SH, Sivabalan R, Arabindoo B, Murugesan V. Agriculture solid waste for the removal of organics adsorption of phenol from water and wastewater by palm seed coat activated carbon. Waster Manage. 2002; 22: 543–548.
8. Busca G, Berardinelli S, Resini C, Arrighi L. Technologies for the removal of phenol from fluid streams. J Hazard Mater. 2008; 160: 265–288. doi: 10.1016/j.jhazmat.2008.03.045 PMID: 18455866
9. Das S, Banthia AK, Adhikari B. Porous polyurethane urea membranes for pervaporation separation of phenol and chlorophenols from water. Chem Eng J. 2008; 138: 215–223.
10. Banerji SK, Bajpai RK. Cometabolism of pentachlorophenol by microbial species. J Hazard Mater. 1994; 39: 19–31.
11. Graham N, Chu W, Lau C. Observation of 2, 4, 6-trichlorophenol degradation by ozone. Chemosphere. 2003; 51: 237–243. doi: 10.1016/S0045-6535(02)00815-9 PMID: 12604075
12. Dąbrowski A, Podkościelny P, Hubicki Z, Barczak M. Adsorption of phenolic compounds by activated carbon-a critical review. Chemosphere. 2005; 58: 1049–1070. doi: 10.1016/j.chemosphere.2004.09.067 PMID: 15664613
13. Karthikeyan T, Rajgopal S, Miranda LR. Chromium (VI) adsorption from aqueous solution by *Hevea brasilinesis* sawdust activated carbon. J Hazard Mater. 2005; 124: 192–199. doi: 10.1016/j.jhazmat.2005.05.003 PMID: 15927367
14. Kavitha D, Namasivayam C. Experimental and kinetic studies on methylene blue adsorption by coir pith carbon. Bioresour Technol. 2007; 98: 14–21. doi: 10.1016/j.biortech.2005.12.008 PMID: 16427273

15. Lim WC, Srinivasakannan C, Balasubramanian N. Activation of palm shells by phosphoric acid impregnation for high yielding activated carbon. J Analy Appl Pyrol. 2010; 88: 181–185.
16. Wang K, Cai J, Feng J, Xie SL. Phytoremediation of phenol using *Polygonum orientale*, including optimized conditions. Environ Monit Assess. 2014; 186: 8667–8681. doi: 10.1007/s10661-014-4034-9 PMID: 25208519
17. Wang L, Zhang J, Zhao R, Zhang CL, Li C, Li Y. Adsorption of 2, 4-dichlorophenol on Mn-modified activated carbon prepared from *Polygonum orientale* Linn. Desalination. 2011; 266: 175–181.
18. Haukos DA, Smith LM. Moist-soil management of playa lakes for migrating and wintering ducks. Wildl Soc Bull. 1993; 21: 288–298.
19. Yang ZY, Qin MJ, Qian SH. Advances in study on *Polygonum orientale* L. Chinese Wild Plant Resour. 2008; 27: 11–15.
20. Ferrero A, Vidotto F, Ug UU. Development of Polygonum orientale L. grown in competition with maize (Zea mays L). In: Trans W. Fac Landbouwkundige Toegepaste Biol 50th International Symposium on Crop Protection. Ghent: Universiteit Gent; 1998.p. 833–838.
21. Boehm HP. Some aspects of the surface chemistry of carbon blacks and other carbons. Carbon. 1994; 32: 759–769.
22. Kalavathy MH, Karthikeyan T, Rajgopal S. Kinetic and isotherm studies of Cu (II) adsorption onto H_3PO_4-activated rubber wood sawdust. J Colloid Interf Sci. 2005; 292: 354–362.
23. Ho YS, McKay G. Pseudo-second order model for sorption processes. Process Biochem. 1999; 34: 451–465.
24. Weber WJ, Morriss JC. Kinetics of adsorption on carbon from solution. J Sanit Eng Div Am Soc Civil Eng. 1963; 89: 31–60.
25. Kannan N, Sundaram MM. Kinetics and mechanism of removal of methylene blue by adsorption on various carbons-a comparative study. J Dyes Pig. 2001; 51: 25–40.
26. Langmuir I. The adsorption of gases on plane surfaces of glass, mica and platinum. J Am Chem Soc. 1918; 40: 1361–1403.
27. Weber TW, Chakkravorti RK. Pore and solid diffusion models for fixed bed adsorbers. Am Inst Chem Eng J. 1974; 20: 228.
28. Freundlich H. Adsorption in solution. Phys Chem Soc. 1906; 40: 1361–1368.
29. Gupta VK, Mittal A, Krishnan L, Gajbe V. Adsorption kinetics and column operations for the removal and recovery of malachite green from wastewater using bottom ash. J Sep Purif Technol. 2004; 40: 87–96.
30. Sathishkumar M, Binupriya AR, Kavitha D, Yun SE. Kinetic and isothermal studies on liquid-phase adsorption of 2, 4-dichlorophenol by palm pith carbon. Bioresour Technol. 2007; 98: 866–873. doi: 10.1016/j.biortech.2006.03.002 PMID: 16678406
31. Rajeshwarisivaraj S, Sivakumar P, Senthilkumar V, Subburam R. Carbon from cassava peel, an agricultural waste, as an adsorbent in the removal of dyes and metal ions from aqueous solution. Bioresour Technol. 2001; 80: 233–235. PMID: 11601548
32. Wang L, Zhang J, Zhao R, Li Y, Li C, Zhang CL. Adsorption of Pb (II) on activated carbon prepared from *Polygonum oriental* Linn: kinetics, isotherms, pH, and ionic strength studies. Bioresour Technol. 2010; 101: 5808–5814. doi: 10.1016/j.biortech.2010.02.099 PMID: 20362430
33. Aguilar C, Garca R, Soto-Garrido G, Arriagada R. Catalytic wet air oxidation of aqueous ammonia with activated carbon. Appl Catal B. 2003; 46: 229–237.
34. Guo J, Lua AC. Textural and chemical properties of adsorbent prepared from palm shell by phosphoric acid activation. Mater Chem Phys. 2003; 80: 114–119.
35. Abdel-Nasser A, El-Hendawy AA. Influence of HNO_3 oxidation on the structure and adsorptive properties of corncob-based activated carbon. Carbon. 2003; 41: 713–722.
36. Özer A, Akkaya G. The removal of Acid Red 274 from wastewater: combined biosorption and biocoagulation with Spkogyra rhizopus. J Dyes Pig. 2006; 7l: 83–89.
37. Garg VK, Kumar R, Gupta R. Removal of malachite green dye from aqueous solution by adsorption using agro-industry waste: a case study of *Prosopis cineraria*. J Dyes Pig. 2004; 62: 1–10.
38. Moreno-Castilla C. Adsorption of organic molecules from aqueous solutions on carbon materials. Carbon. 2004; 42: 83–94.
39. Mall D, Srivastava VC, Agarwal NK, Mishra IM. Adsorptive removal of malachite green dye from aqueous solution by bagasse fly ash and activated carbon-kinetic study and equilibrium isotherm analyses. J Colloid Surf A. 2005; 264: 17–28.

40. Nakbanpote W, Thiravetyan P, Kalambaheti C. Preconcentration of gold by rice husk ash. Miner Eng. 2000; 13: 391–400.
41. Lützenkirchen J. Ionic strength effects on cation sorption to oxides: macroscopic observations and their significance in microscopic interpretation. J Colloid Interf Sci. 1997; 195: 149–155.
42. Chen L, Wang XK. Influence of pH, soil humic/fulvic acid, ionic strength and foreign ions on sorption of thorium (IV) onto (-Al_2O_3). Appl Geochem. 2007; 22: 436–445.
43. Wang L, Zhang J, Zhao R, Li C, Zhang CL. Adsorption of basic dyes on activated carbon prepared from *Polygonum orientale* Linn: Equilibrium, kinetic and thermodynamic studies. Desalination. 2011; 254: 68–74.
44. Pavan F, Dias S, Lima E, Benvenutti E. Removal of Congo red from aqueous solution by anilinepropyl-silica xerogel. J Dyes Pig. 2008; 76: 64–69.
45. Vimonses V, Lei S, Jin B, Chow C, Saint C. Kinetic study and equilibrium isotherm analysis of Congo red adsorption by clay materials. Chem Eng J. 2009; 148: 354–364.
46. Wu C, Tseng RL, Juang RS. Comparisons of porous and adsorption properties of carbons activated by steam and KOH. J Colloid Interf Sci. 2005; 283: 49–56.
47. Poots VJP, McKay G, Healy JJ. Removal of basic dye from effluent using wood as an adsorbent. J Water Pollut Control Fed. 1978; 50: 926–939.
48. Cheung WH, Szeto YS, McKay G. Intraparticle diffusion processes during acid dye adsorption onto chitosan. Bioresour Technol. 2007; 98: 2897–2904. doi: 10.1016/j.biortech.2006.09.045 PMID: 17110098